



An integration of the numerical and soft computing approaches for determining inflow control device flow area in water injection wells

Farshad Mostakhdeminhosseini¹ · Yousef Rafiei¹

Received: 22 July 2023 / Accepted: 8 March 2024
© The Author(s) 2024

Abstract

To avoid or mitigate the unwanted water and gas content, inflow control devices (ICDs) are designed and installed in the well to disturb the water and gas breakthrough which are trying to overtake the oil inflow, water and gas coning and sand production. Smart wells with permanent downhole valves such as ICDs are used to balance production and injection in wells. A paramount issue regarding using downhole control devices is determining the required cross-sectional area of them for control of the imposed pressure drop across the device to stabilize the fluid flow. Current methods for calculating the opening size of the ICDs are mainly based on sensitivity analysis of the ICD flow area or optimization algorithms coupled with simulation models. Although these approaches are quite effective in oil field cases, they tend to be time-consuming and require demanding system models. This paper presents a fast analytical method to determine the ICD flow area validated by a genetic algorithm (GA). Analytically, a closed-form expression is introduced by manipulating Darcy's law applicable to multi-layer injection wells with different layer properties to balance the injection profile in the reservoir pay zone, based on equalizing injected front velocity in layers with different permeability. Considering various scenarios of analytical technique, GA optimization, and sensitivity analysis scenarios for ICD cross-sectional area determination, results for oil recovery, water production, water breakthrough time, and net present value (NPV) are discussed and compared. NPV values obtained by both analytical and GA approaches are virtually identical and greater than those of other scenarios. Compared to the base field case, the analytical method improved the oil recovery by almost 1%, reduced water production by almost 91%, and synchronized the water breakthrough time of high- and low-permeability layers (from a ratio of 1.76–1.06). The proposed analytical solution proved to be capable of providing desirable results with only one reservoir simulation run in contrast to GA and sensitivity analysis scenarios which require iterative simulation runs. The proposed analytical solution outperformed the GA as it is less computationally demanding in addition to its success in case of lowering water production for the field data. The findings of this study can help for a better understanding of the situation where water injection into the oil reservoir is problematic as the layers present different permeabilities which can induce problems such as early water breakthrough from the more permeable layer and hinder the success of the water injection process. Using ICDs and a faster and more accurate approach to calculate its cross-sectional area such as the analytical method that was used in this study can greatly increase the success rate of water injection in case of oil recovery and lower the amount of the produced water.

Keywords Inflow control device flow area · Artificial intelligence · Improved oil production · Water breakthrough time

List of symbols

Latin letters

A	Cross-sectional area of each layer (ft ²)
A_c	ICD cross-sectional area (ft ²)
A_p	Well cross-sectional area (ft ²)

B	Formation volume factor (bbl/STB)
C_0	Constant cost (\$)
C_v	ICD constant (\$)
D	Well diameter (ft)
f	Fanning friction factor
h_i	Is the thickness of layer i (ft)
k_i	Permeability of layer i (md)
P_e	Reservoir external pressure (psi)
P_{eq_i}	Wellbore pressure after ICD insertion (psi)
P_{wi}	The bottom-hole injection pressure for layer i (psi)

✉ Yousef Rafiei
y.rafiei@aut.ac.ir

¹ Department of Petroleum Engineering, Amirkabir University of Technology, Tehran, Iran

Q_g	Gas production rate (MSCF/Day)
q_i	Injection flow rate in layer i (ft^3/Day)
Q_i	Water injection rate (STB/Day)
Q_o	Oil production rate (STB/Day)
q_{total}	Surface injection rate (ft^3/Day)
Q_w	Water production rate (STB/Day)
r	Front radius of injected water (ft)
r_e	Reservoir radius (ft)
r_g	Cost of gas handling (\$)
r_i	Cost of injected water (\$)
r_o	Oil price (\$)
r_w	Cost of water handling (\$) or wellbore radius
S_i	Skin factor of the wellbore in contact with the layer
t_k	Time (year)

Greek letters

ΔP_i	Pressure difference in layer i (psi)
ΔP_{valve}	Pressure-drop across ICD (psi)
ρ	Fluid density (lb_m/ft^3)
μ	Fluid viscosity (cp)

Abbreviations

AFCD	Autonomous Flow Control Device
AI	Artificial Intelligence
AICD	Autonomous Inflow Control Device
AICV	Autonomous Inflow Control Valve
CF	Cross Over Factor
CFD	Computational Fluid Dynamics
GA	Genetic Algorithm
ICD	Inflow Control Device
ICV	Inflow Control Valve
MF	Mutation Factor
NPV	Net Present Value
SSMQN	Single Shooting Multi-Step Quasi-Newton

Introduction

Energy demand is increasing in the world, and fossil fuel is still one of the main energy resources. As a vast majority of oil fields are in the second half of their life, enhancing oil recovery in such fields is of great importance, which can be carried out using leading-edge technologies in this regard. Water injection is one of the most popular and common options for improving oil recovery (Kalam et al. 2022) because of its availability, relative ease of injection, good dispersivity in oil formations, and productivity associated with oil displacement (Asadollahi 2012). This, in turn, contributes to reservoir pressure maintenance together with oil displacement toward the producing interval. Having said that, water injection may cause early water breakthrough in high-permeability layers as well (Rafiei 2014). Discrepancy in layer properties of a multi-layer reservoir may impede

water flooding performance. Speedy movement of injected water through the layer with higher permeability causes premature water breakthrough and excessive water production. Thus, after some years, production will no longer be economically viable, and producing well will be shut down (Mohammadpourmarzbali et al. 2019). In this work, a mathematical procedure is developed to design oil wells in an optimum way with the end goal of increasing oil production and postponing water breakthrough.

Smart wells are unconventional types of wells with downhole devices including sensors and specific valves controlling the flow rate known as control valves. These wells also allow real-time monitoring of fluid flow rate, pressure, and adjustment of downhole valves. Smart well technology provides high flexibility in the operation of multi-layer reservoirs so that each layer can be controlled individually. This technology also integrates regional production management by virtue of control valves and proper flow monitoring equipment to improve well and oilfield performance. Regional production management is capable of increasing oil production and/or reducing unnecessary fluid production. Intelligent well control instruments are divided into two categories—passive inflow control devices (ICDs) and active interval control valves (ICVs) (Ebadi and Davies 2006; Gao et al. 2007). ICDs are generally preferred to ICVs owing to their lower expense, lower complexity, and long-term durability (Rahimbakhsh and Rafiei 2018). However, in general, ICV's applicability has been investigated to be successful in real-case scenarios (Ahn et al. 2023). Moreover, autonomous flow control devices (AFCDs) are introduced as a means of controlling unwanted phases' production (gas/water) (Eltaher et al. 2019). An autonomous inflow control device (AICD) takes advantage of both active and passive control, providing a pressure drop dependent on flowing fluid properties and rate. Also, the autonomous inflow control valve (AICV) poses an increased pressure drop (due to flow into the by-pass module), controlling the unwanted fluid flow rate. According to experience, smart valves' ability to increase production depends on factors such as porosity and permeability distribution in the reservoir layer; hence, heterogeneous reservoirs, which are broadly observed with the early breakthrough of the injection fluid, are the best candidates for intelligent well completions (Ebadi et al. 2005). In case of permeability differences between different layers, fluid flow will be partitioned across them and lower permeability region will be bypassed, which is a concern in various areas of engineering involving stratified porous media such as tracer dispersion. For example, Dejam and Hassanzadeh derived a reduced-order model for tracer dispersion in stratified porous media by generalizing the Taylor dispersion theory and Stokes flow in porous media (Dejam and Hassanzadeh 2022). Shale reservoirs are great examples of heterogeneous structures (Li et al. 2017). By

their local climate, deposition, and diagenesis variety, shale reservoirs have inhomogeneous characteristics in the case of internal properties and spatial distribution (Xiaorong et al. 2016). Also shale layers due to their dense texture and low permeability can introduce severe heterogeneities when they are in the vicinity of a more permeable layer (Dan et al. 2015).

As mentioned earlier, one of the severe challenges in water injection scenarios is early water breakthrough in highly conductive layers. To tackle this issue, ICDs have been employed as a potentially viable solution to curb early water breakthroughs from so-called “guilty” intervals. Improper design of the ICD not only fails to control the fluid flow rate but also increases operating costs. For this purpose, controlling and determining the flow cross-sectional area is one of the most important factors in ICDs’ design.

Regarding implementing intelligent well completions in petro physically heterogeneous reservoirs, several research studies have been done which are reviewed as follows. Brouwer et al. (2001) managed water injection into a field with a high degree of heterogeneity using a horizontal injection well by employing a genetic algorithm (GA) method. Pressure and rate data for each well segment were taken as input data for the GA working based on optimizing the productivity index for each well section. Downhole control valves were also used during water injection operations for the sake of preventing early water breakthrough and reaching optimal production possibilities. The only function of the downhole control valve used was to open and close logical operators. Meum et al. (2008) investigated the ICV adjustment by using the single shooting multi-step quasi-Newton (SSMQN) method in which the objective function was oil recovery. Additionally, Al-Ghareeb, (2009) applied GA to optimize ICVs’ settings in a naturally fractured reservoir. Objective functions included minimizing water cut, extending production plateau, and maximizing net present value (NPV). Wang et al. (2016) developed a coupled model of reservoir-ICD-wellbore to take account of bottom water in heterogeneous reservoirs. They found water coning to be delayed using ICD. Zhang et al. (2019), also, proposed a new AICD model accounting for bottom water as well as solid particles in loose sands using computational fluid dynamics (CFD). In our study, the heterogeneity considered is the layered nature of the reservoir in which reservoir layers can be of their petrophysical properties.

As for quantifying the smart wells’ profitability, several ICD/ICV size determination methods have been introduced and proved to be helpful in practice. Cullick and Sukkestad (2010) investigated the purpose served by smart wells in a multi-branch horizontal production well. They made use of Perkins (1993) model (sub-critical pressure drop across ICV) to find the size of the ICV and predicted pressure drop across the valve. Cullick and Sukkestad assumed that

the inflow control valve acts as a choke, and set the goal of maximizing oil production. Their methodology was based on simulation analysis and automated procedures to optimize the objective function. Meshioye et al. (2010) found the optimal injection rate to each layer using the set-point optimization method combined with numerical reservoir simulation. The optimization process was conducted in three sample cases of a three-layer reservoir with different characteristics. ICV valves were used to delay water breakthrough time, and the objective function was to reach the maximum oil recovery or the highest NPV. Li et al. (2011) generated a flow profile of a horizontal well by using an inflow-outflow method through which additional frictional pressure drops created by ICDs were also considered. They used a general, empirical equation for the ICD pressure drop, and skin factor was included in the ICD pressure drop as well. Hassanabadi et al. (2012) optimized ICDs’ port sizes with a particle swarm optimization algorithm via neural network modeling to maximize oil production. Behrouz et al. (2016) proposed a workflow to determine the cross-sectional area of the ICV based on its effect on predefined target performance. Their workflow starts with a predefined ICV area at a fully open position. Based on the trial-and-error method, the workflow selects the size of the cross-sectional area of the valve. The target considered in the study by Behrouz et al. was an increment in total oil output and diminishing water production. Chen and Reynolds (2017) ran the EnOpt algorithm (an ensemble-based optimization technique) to simultaneously optimize well control (rate/pressure) and ICV setting in a case of water alternating gas (WAG) injection with NPV as the objective function. Lee et al. (2017) studied the effect of ICD regulation on flux equalization and well productivity reduction. They used various cases of well productivity index and permeability changes enabling the operator to calculate the required ICD strength or number of ICD joints along the well to maximize the recovery factor. Being a time-consuming simulation process, only the fast close wellbore simulation was used to design ICD completions. Ugwu and Moldestad (2018) numerically simulated a case study with reservoir conditions alike the Troll offshore Norway using the ICD via Eclipse reservoir simulator. The early breakthrough time for water and gas in their study was delayed and gas production was reduced by 51% with ICD completion. Prakasa et al. (2019) developed a fully analytical workflow (assisted by type curve matching) for ICD completions of both homogeneous and heterogeneous reservoirs producing via horizontal wells. Although, in terms of computational efficiency, such a fully analytical method proves beneficial, its practicality for real-world scenarios, which are broadly in need of numerical reservoir simulation, may be questionable. Also, in some cases of their study, their proposed model had no improvement in the oil production rate compared to empirical

models. Moradi and Moldestad (2020) simulated near-wellbore oil production of a horizontal well by applying ICD and AICD completions using OLGa and ROCX packages. An empirical equation was utilized to calculate the ICD pressure drop dependent on the flow rate, valve geometry, and fluid density. By using these downhole control devices, water breakthrough time was delayed, accumulated water production was reduced, and cost-effective oil production was achieved. As for handling massive computations relevant to multilateral well completion fluid dynamics, Aljubran and Horne (2020) showed how a machine learning approach (coupled with reservoir simulation) can optimally design ICV settings over time to maximize well production for both homogenous and heterogeneous reservoirs. Zhang et al. (2021) employed a multi-objective optimization algorithm to obtain optimal ICD configuration for a horizontal well. Determining the ICD location and nozzles' number and size yielded production rate and water breakthrough time to occur optimally. Sabet et al. (2022), took advantage of both CFD and empirical correlations to describe ICD characteristics. Using correlations based on CFD results, their work can provide operators with easy-to-use formulae flexible about well/reservoir conditions. Recently, Rezvani and Rafiei (2023) presented an analytical approach for ICD flow area using the velocity equalization concept for injection host layers for CO₂-EOR applications. They showed their model is capable of postponing injected CO₂ breakthrough time. However, their study was not accompanied by layer-based gas breakthrough insights, and it was shown that total gas breakthrough was delayed by their proposed method. We, also, published premier findings of our study on ICD cross-sectional area quantification using an analytical formulation in conference proceedings (Mostakhdeminhosseini et al. 2020). In that study, the obtained analytical formulation ran for a field case and was compared to a no-control scenario. The results showed its suitability for improving oil recovery as well as delaying early well water production.

Having discussed the relevant literature to our study, distinctions of this study in comparison with the literature should be outlined. Firstly, no research to date has considered the concept of equalizing velocity between oil-producing layers in a water flooding scenario. This leads to the delaying of water breakthrough which will be discussed later in detail. Previous studies for ICD/ICV size determination either use empirical equations (Li et al. 2011; Moradi and Moldestad 2020) or iterative numerical simulations (Behrouz et al. 2016; Chen and Reynolds 2017; Lee et al. 2017; Meshioye et al. 2010; Moradi and Moldestad 2020; Sabet et al. 2022; Ugwu and Moldestad 2018; Zhang et al. 2021) to optimize oil production or NPV. Iterative numerical simulations require a trial and error technique for selecting a valve size through an optimization task which is indeed time-consuming, especially for real-world field scenarios. This determines

how an easy-to-use analytical tool for downhole control devices' size determination can be useful for operators and engineers. Such an analytical tool is to be time-saving for further reservoir simulation computations. Secondly, most of the reviewed studies lack observations on all 3 factors of oil production, water breakthrough time, and NPV. Cullick and Sukkestad (2010), Hassanabadi et al. (2012), and Prakasa et al. (2019) had no study on water breakthrough time, (Aljubran and Horne 2020; Cullick and Sukkestad 2010; Lee et al. 2017; Zhang et al. 2021) did not consider NPV in their optimizations. In this study, we present our findings not only on oil production optimization but also on water breakthrough time and NPV maximization.

In this study, an analytical method is proposed for computing proper ICDs' flow cross-sectional area. This exact solution, needing only basic reservoir properties of each layer together with well operational parameters (more importantly surface injection flow rate), is able to determine the ICD flow area in a fast way. On the other hand, there are other approaches available such as artificial-intelligence (AI)-based and sensitivity-analysis-based methods which are relatively computationally demanding. Both of these approaches are compared with our analytical model in this study. The workflow suggested in this study starts with reservoir simulation of the concerned injection-production scenario coupled with either our proposed analytical model or AI-based (GA here) methods (see Fig. 1) for ICD cross-sectional area determination. Having been determined, a comparison can be made by the user to select the most efficient method in terms of simulating production and recovery factor increase, water breakthrough delay, and water cut reduction based on reservoir simulation results. Recall that neither GA nor sensitivity analysis cases were covered in our study presented before (Mostakhdeminhosseini et al. 2020). The core of the analytical formulation of this study originates from equalizing fluid velocity in high- and low-permeability layers of a two-layer production interval, and deriving the ICD cross-sectional area based on that. By reducing the fluid velocity in the highly permeable layer, the water breakthrough time in this layer is reduced to the water breakthrough time of the low-permeability layer. This way, water breakthrough times in these two layers are synchronized, which is advantageous for oil production and the NPV of the field. The novelty of our work lies in the analytical method that is based on the idea of eliminating the early water breakthrough issue by adjusting the water injection rate into different layers with different petrophysical properties which was never done to the extent of our knowledge. This analytical solution is advantageous in the case of computational time which is much faster than the other methods alongside its ability to rectify early water production which strongly determines the success of the water injection technique. This advantageous analytical solution is applicable in oil reservoirs and in the case of other types of

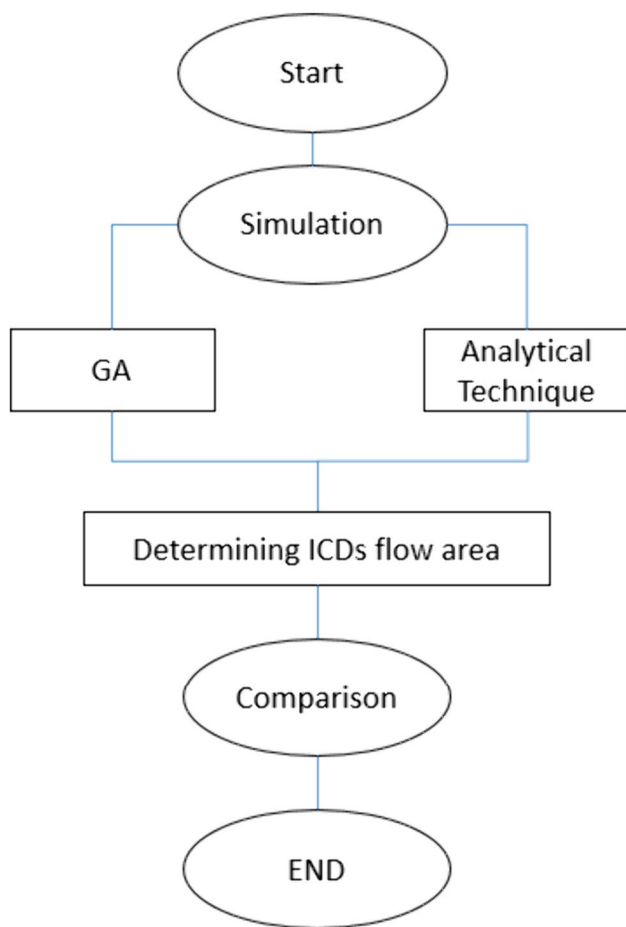


Fig. 1 Workflow proposed for determining ICDs cross-sectional area in this study

reservoirs needs some adjustments which can be named as its limitation which also can be a potential extension to this work that can broaden its applicability.

Methodology

Analytical methods to determine the cross-sectional area of ICDs as well as a GA approach are introduced in this section. Analytical methods are widely accepted owing to their computational efficiency and flexibility compared to numerical counterparts (Chu et al. 2023; Dutt and Mandal 2012; Wang et al. 2021). A schematic workflow of the proposed methodology for determining ICDs' flow area is as Fig. 1. According to this flowchart, numerical reservoir simulation is set to run for any consecutive injection-production scenario while coupled with either analytical method or GA to determine ICDs' flow area through which the simulation results can be compared together. Entries of GA from reservoir simulation are oil and water production rate plus water injection rate, whereas the latter works

iteratively to reach the optimum ICD size and requires multiple simulation runs, the former is quite straightforward and runs only one time considering the ICD size from analytical formulation. This way, one can investigate to what extent each of these methods is successful for ICD flow area determination in terms of increasing hydrocarbon production and tackling water breakthrough and early production issues.

Analytical technique

To begin with, the physical concept behind the formulae of the analytical method derivation should be clarified. To delay water breakthrough time—an important monitoring parameter of water flooding (Huang et al. 2019)—, the fluid front movement must be balanced in layers with different permeability values. Fluid velocity in the high-permeability layer should be reduced to that of the low-permeable layer. Accordingly, a piston-like movement is achieved and the injection fluid front in both layers reaches the production well at the same time leading to delaying the water breakthrough.

According to Eq. (1), layer velocity is equal to the flow rate divided by the cross-sectional area of the corresponding layer.

$$V_1 = V_2 \Rightarrow \frac{q_1}{A_1} = \frac{q_2}{A_2} \quad (1)$$

where V_1 , V_2 , q_1 , q_2 , A_1 , and A_2 are the velocity, flow rate, and cross-sectional area of the fluid flow in layer 1 and layer 2, respectively.

The general form of the injection inflow equation from well to reservoir is as Eq. (2) (Ahmed 2018):

$$q_i = \frac{k_i h_i}{141.2 \times \mu B \times \left(\ln \left(\frac{r_e}{r_w} \right) + S_i \right)} (\Delta P_i + \Delta P_{\text{VALVE}}) \quad (2)$$

where q_i is the injection flow rate in layer i , h_i is the thickness of layer i , k_i permeability of layer i , S_i is the skin factor of the wellbore in contact with layer i , and ΔP_i and ΔP_{valve} denote pressure difference in layer i and pressure-drop across the ICD, r_e and r_w are reservoir and wellbore radius, μ is fluid viscosity and B is formation volume factor, respectively. As for conciseness, units of all computational parameters are summarized in the nomenclature section.

The term ΔP_i is calculated as the difference between reservoir external pressure (P_e) and wellbore pressure (P_{wi}) for layer i . The pressure-drop term across the ICD is as Eq. (3):

$$\Delta P_{\text{VALVE}} = P_{wi} - P_{\text{eq}_i} \quad (3)$$

where P_{wi} is the bottom-hole injection pressure for layer i and P_{eq_i} is wellbore pressure after ICD insertion.

In a hypothetical two-layer reservoir with different thicknesses and permeabilities (see Fig. 2), ICD is placed in the layer with higher permeability (layer 1). The injection inflow equation from well to reservoir is written down in Eq. (4) for layer 1 and in Eq. (5) for layer 2.

$$q_1 = \frac{k_1 h_1}{141.2 \times \mu B \times \left(\ln \left(\frac{r_e}{r_w} \right) + S_1 \right)} (P_{eq_1} - P_e) \tag{4}$$

$$q_2 = \frac{k_2 h_2}{141.2 \times \mu B \times \left(\ln \left(\frac{r_e}{r_w} \right) + S_2 \right)} (P_{w_2} - P_e) \tag{5}$$

By substituting Eqs. (4) and (5) into Eq. (1) one can have Eq. (6) as:

$$V_1 = V_2 \Rightarrow \frac{q_1}{A_1} = \frac{q_2}{A_2} \Rightarrow \frac{k_1 h_1}{A_1} (P_{eq_1} - P_e) = \frac{k_2 h_2}{A_2} (P_{w_2} - P_e) \tag{6}$$

where A for both layers 1 and 2 can be quantified as shown in Eq. (7).

$$A_1 = 2\pi r_1 h_1 \text{ and } A_2 = 2\pi r_2 h_2 \tag{7}$$

A_1 and A_2 are the cross-sectional areas of two layers in which injected waterfront moves, and r_1 and r_2 are the front radius of injected water in two layers.

These two front radii of injected water in two layers (r_1 and r_2) must be equal since the fluid velocity has to be identical in these layers. As such, Eq. (8) derives how the flow rate in these two layers can be related:

$$V_1 = V_2 \Rightarrow r_1 = r_2 \Rightarrow q_1 = \frac{h_1}{h_2} q_2 \tag{8}$$

Considering this relationship between the two layers' flow rate, the total flow rate is determined as follows in Eq. (9).

$$q_{total} = q_1 + q_2 = \left(\frac{h_1 + h_2}{h_2} \right) q_2 \tag{9}$$

According to Eq. (9) and having the surface injection rate (q_{total}) known, one can determine the downhole injection rate for each layer (q_1 and q_2).

Determining P_{eq_1} from Eq. (6) combined with Eq. (3), the ICD pressure difference can be derived as Eq. (10) below:

$$\Delta P_{VALVE} = P_{w_1} - \left(\frac{k_2}{k_1} (P_{w_2} - P_e) + P_e \right) \tag{10}$$

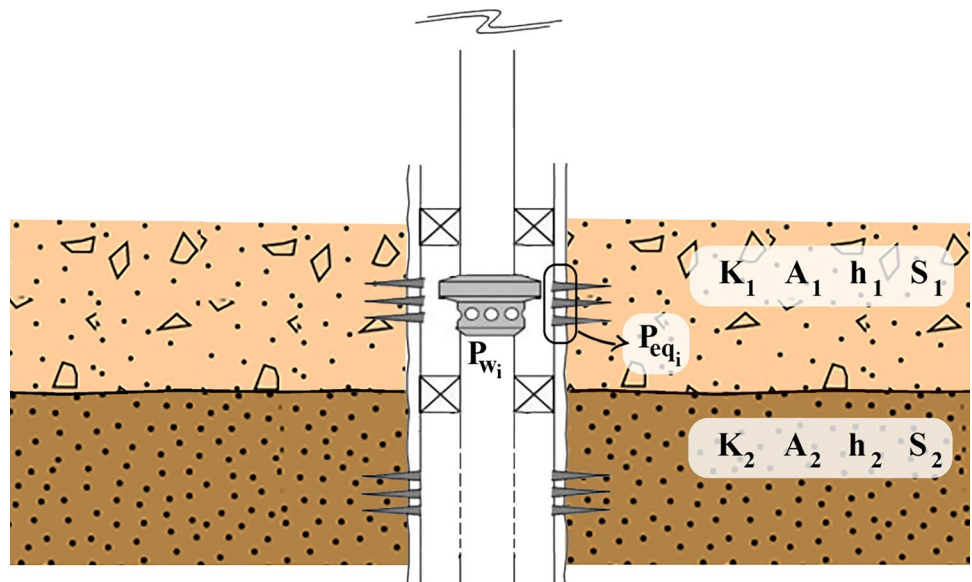
The ICD pressure-drop equation is also calculated from the following equation (Eq. 11) (Schlumberger 2010):

$$\Delta P_{VALVE} = C_u \frac{\rho \left(\frac{q_i}{A_c} \right)^2}{2C_v^2} + 2C_u f \frac{L}{D} \rho \left(\frac{q_{total}}{A_p} \right)^2 \tag{11}$$

where C_u is a constant coefficient, C_v is ICD constant, A_c is ICD cross-sectional area, A_p is well cross-sectional area, D is well diameter, f is fanning friction factor, and ρ is fluid density.

Therefore, Eq. (12) in the following is obtained to calculate the cross-sectional area of the ICD:

Fig. 2 Schematic profile view of a two-layer reservoir with ICD installed in the high-permeability layer



$$A_c = \sqrt{\frac{\frac{C_u \rho q_i^2}{2C_v^2}}{P_{w_1} - \left(\frac{k_2}{k_1}(P_{w_2} - P_e) + P_e\right) - 2C_u \frac{fL\rho q^2}{DA_p^2}}}} \quad (12)$$

Genetic algorithm approach

Genetic algorithm (GA) is accounted as an evolutionary AI-based algorithm in terms of evaluating complex engineering problems. This algorithm initiates by producing an initial random solution (chromosomes) and reproducing it iteratively to converge to the optimum solution of the problem (Mohammadi Behboud et al. 2023). Reproduction is implemented through crossover and mutation operations. The crossover factor (CF) is defined as the probability of offspring production by chromosomes' pairs, and the mutation factor (MF) is the probability of binary chromosome pairs if they change from 0 to 1. Optimization through GA can be achieved following the below procedure (Alam et al. 2015; Karkevandi-Talkhoonchek et al. 2017):

1. Setting initial chromosomes, CF and MF.
2. Quantifying objective function (fitness of chromosomes), and finding the best chromosomes.
3. Selecting chromosomes, parents' crossover and offspring mutation to have new chromosomes.
4. Evaluating objective function whether the propriety criteria are fulfilled.
5. If the solution is not proper, the iteration process reverts to step 3; if the solution is proper (or the maximum iteration number is reached), the optimum solution is obtained.

Here, GA works in parallel with the reservoir model running in the commercial reservoir simulator to optimize NPV—the difference between present cash inflow/outflow (Taghavinejad et al. 2022). Equation (13) serves as the objective function of the optimization problem using GA, and the cross-sectional area of the valve is the main variable in this problem.

$$NPV = \sum_{K=1}^M \frac{Q_o r_o - Q_w r_w - Q_g r_g - Q_i r_i}{(1+b)^{t_k}} - C_o \quad (13)$$

where Q_o , Q_w , Q_g , and Q_i refer to oil production rate, water production rate, gas production rate, and water injection rate, respectively; r_o , r_w , r_g , and r_i denote oil price, cost of water handling, cost of gas handling, and cost of injected water, respectively; b is the annual discount rate, C_o is constant cost, and t_k is time in a year.

Considering the workflow shown in Fig. 1, reservoir simulation computations are coupled with the GA to select

the best ICD flow area among a range for that. In this respect, the injection-production scenario (compared with other scenarios discussed later in this study) is run, and the optimal amount of cross-sectional area of the valve is calculated via GA. For this goal and according to Eq. (13) as the objective function of GA optimization, the oil price is taken as 50 \$/STB, the annual discount rate is taken as 0.1, and the overall water handling/injection price is taken as 5 \$/STB. It is noteworthy that there is no gas in the production system, the constant cost is zero to make comparisons easier, and production rates and time are taken from the results of reservoir simulation.

GA is implemented considering 50 iterations with CF=0.8, MF=0.05, and a population size of 4. Using a commercial genetic algorithm toolbox and a text editor for coupling that with reservoir simulator input (for manipulation of the ICD flow area), reservoir simulation is run and production/injection rates as well as run time are obtained for NPV calculation (Eq. 13). Until reaching a maximum for the NPV, GA progresses to change the ICD flow area in the reservoir simulation input. The GA optimization result for the field case described later is the ICD flow area equal to 0.00034 ft².

Field application

The field case oil reservoir of this study is in southwestern Iran, and its properties are shown in Table 1. This reservoir is formed from 13 layers, and production occurs from layers 8 and 9. Permeability of layers 8 and 9 are 400 and 800 mD, respectively, as shown in Table 1 and illustrated in Fig. 3. The valve is located in the layer with higher intrinsic permeability (layer 9). The flow rate of the water injected in layer 9 has been controlled by installing ICD to delay the water breakthrough time. The cross-sectional area of the fluid flow has been calculated by the presented analytical equation (Eq. 12) which is equal to 0.000238ft². Also, following the GA approach, the optimum cross-sectional area is determined as 0.00034 ft². Table 1 encompasses the basic reservoir properties of this case study. Also, Fig. 3 illustrates a schema

Table 1 Properties of the studied reservoir model

Parameters	Values
Dimension, ft ³	285 × 65 × 15
Depth, ft	6596
Pressure, psig	4700
Temperature, °F	200
Permeability, mD	Layer 8 = 400
Layer	9 = 800
Porosity, %	25

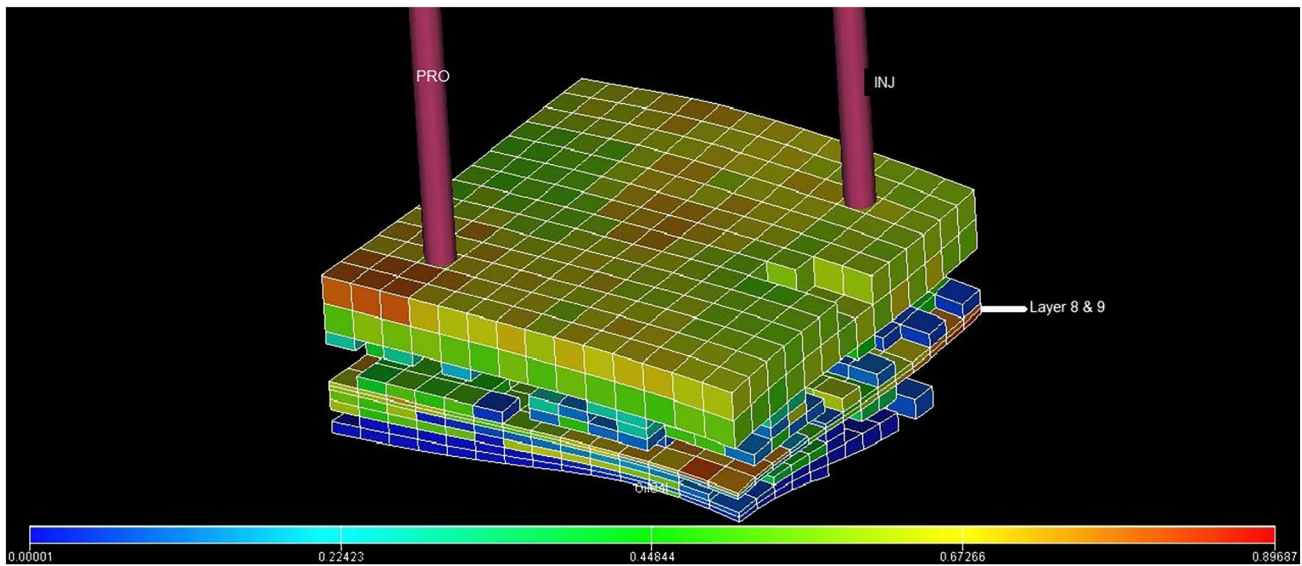


Fig. 3 The reservoir model in this study

of the 3D reservoir model for simulation tasks associated with an injection-production scenario via one injection well and one production well located in the field. The accompanying graphical legend of the reservoir model shows the oil saturation value illustrated by colors (from blue to red) throughout the reservoir grid blocks. In the following, base case scenarios together with other scenarios for ICD flow area determination are introduced.

Base case scenario

A base case scenario is defined based on the maximum performance of the production well and maintaining field pressure. However, in this case, no management of layer-scale water injection is applied, and injection takes place only by its surface control moderation. Production and injection scenarios of this base case are introduced as follows.

Production scenario

As for production from this reservoir, and according to the vertical flow performance (VFP) table of the production well, the minimum allowable wellhead pressure is 150 psi. As a result, the maximum production of the well occurs when the wellhead pressure is 150 psi. A sensitivity analysis of the production rate was performed on the reservoir simulation task to determine the maximum production potential rate. Sensitivity analysis was performed on constrained flow rates of 2000, 2700, and 6000 STB/day. As shown in Fig. 4, the maximum capacity of the well for production proves to be

2700 STB/day whether the production constraint is 2700 STB/day or more.

Injection scenario

The injection flow rate is controlled by voidage replacement meaning that the injection and production volumes would remain identical. Sensitivity analysis was performed on 1500, 2500, 2700, and 3500 STB/day flow rates and 2700 STB/day was selected as a suitable injection rate for the injection well. A comparison of field pressure diagrams plotted in Fig. 5 shows that reservoir pressure falls for cases with injection flow rates of 1500 and 2500 STB/day. Reservoir pressure reduction for the case with 1500 STB/day injection flow rate is remarkably steeper than that of the other one.

Flow-control scenarios

Table 2 presents the field parameters of our analytical equation for moving the injection waterfront at the same velocity as different layers based on the cross-sectional area of the ICDs (0.000238 ft² value as mentioned earlier).

Further discussion on the work will be based on the results of the reservoir simulation using various scenarios of layer-scale injection control. The first scenario would be the base case in which no layer-scale control is considered for water injection. Comparison of all other scenarios with the base case would be meaningful in terms of indicating to what extent they are fruitful for the production system. Analytical technique and GA scenarios are also crucial parts of

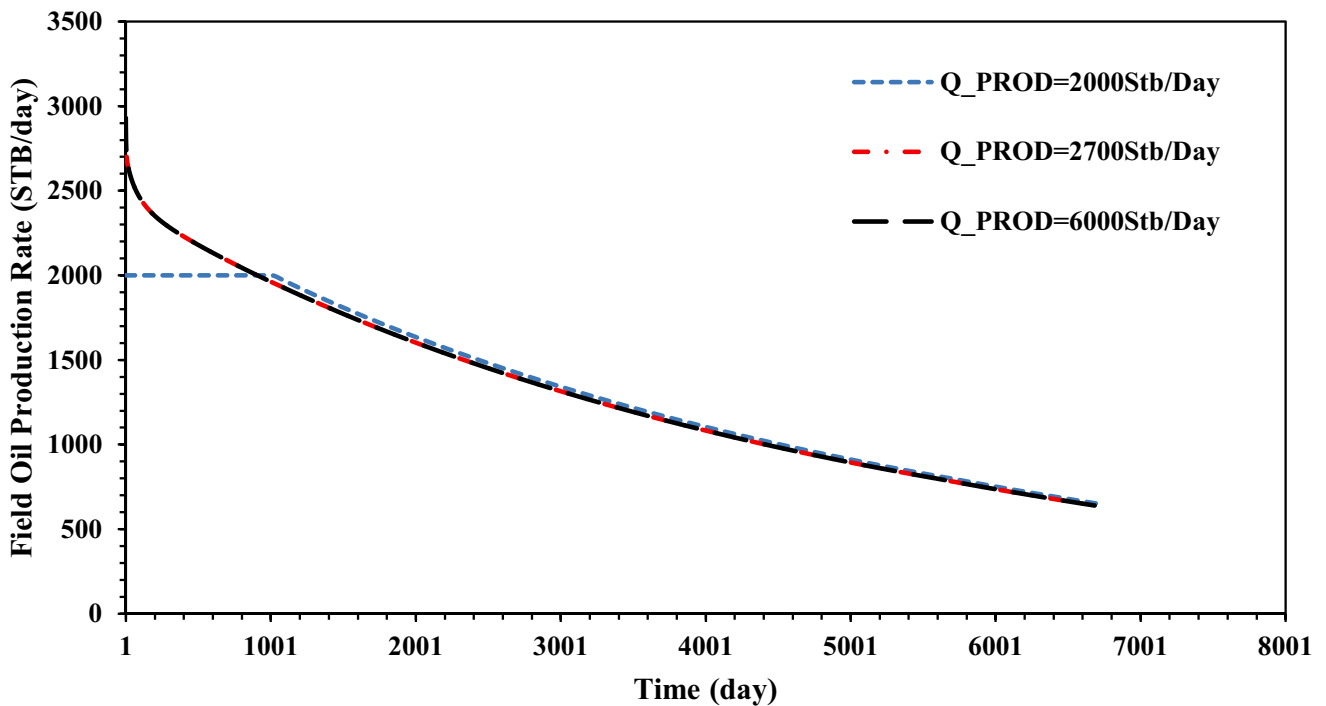


Fig. 4 Sensitivity analysis on field oil production ratio

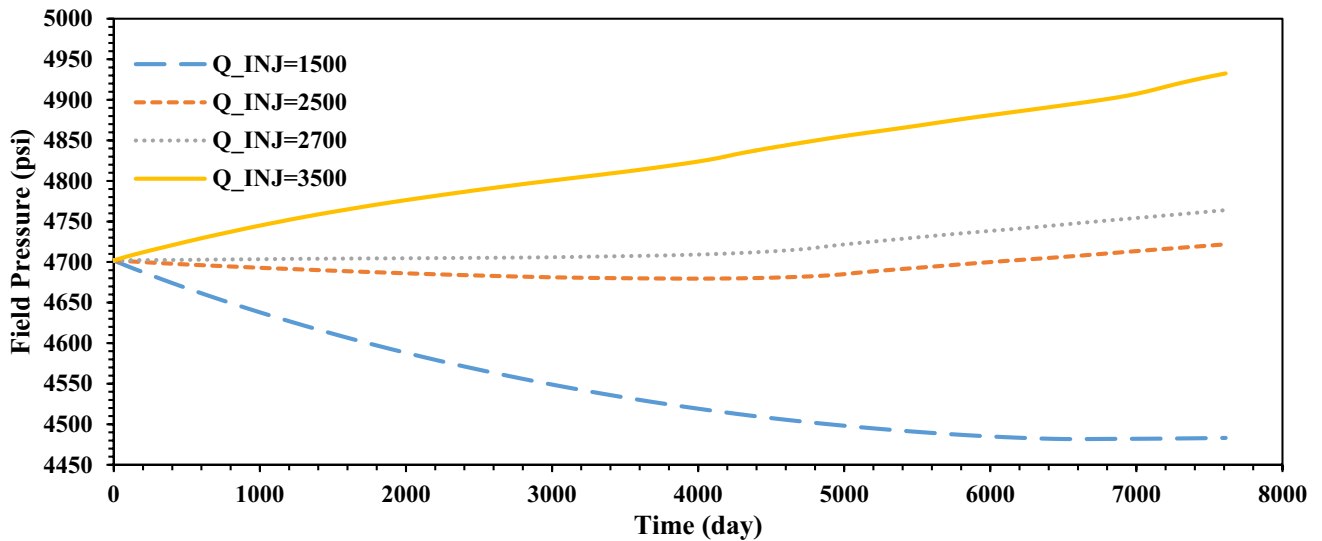


Fig. 5 Comparison of field pressure at different injection rates

the workflow suggested in Fig. 1 thereby one can determine which of these computational methods works better for a specific case. In addition to the three mentioned scenarios, three other scenarios are also considered with fixed values for the ICDs flow area. As a matter of fact, these three cases (cases 4–5 according to Table 3), are sub-cases of a sensitivity analysis by which another meaningful comparison can

be made between their results and those of other scenarios. Making use of sensitivity analysis is quite common in engineering studies of such a case, and benchmarking them along with analytical technique and GA can provide a deep understating of this field study. All considered scenarios whose results are fully discussed in the following section are listed in Table 3.

Table 2 Parameters for valve control using analytical technique

Parameters	Values	Units
ρ	62.428	lb _m /ft ³
P_{w_1}	6100	psi
P_{w_2}	6100	psi
f	0.0015	–
L	15.3	ft
D	0.583	ft
A_p	0.2669	ft ²
A_c	0.000238	ft ²
C_v	0.7	–
C_u	2.89E–14	–
q_i	7018.65	ft ³ /day
K_9 (high-permeability layer)	800	md
K_8	400	md

Table 3 Injection-production scenarios considered

Scenario no	Description
1	Base case
2	Analytical technique
3	GA
4	0.0001 ft ² (ICDs flow area)
5	0.0005 ft ² (ICDs flow area)
6	0.0007 ft ² (ICDs flow area)

Results and discussion

As regards evaluating the efficiency of the analytically derived equation for ICDs' flow area determination (Eq. 12), and for assessing improvement of the water injection process amid the oil production period, results of the proposed analytical method should be compared with results of other scenarios (listed in Table 3). Based on Eq. (12), for calculating the cross-sectional area of the valve, as it was mentioned earlier, the optimum opening of the valve to control the injection flow rate is determined to be 0.000238 square feet for this field case. Figure 6 shows that oil recovery obtained using the analytical model of our study is virtually matched by the GA method, and it is higher than those of other scenarios. It can be implied that by installing a flow control valve with the flow cross-sectional area optimally designed obtained from the analytical equation, the oil recovery factor can significantly increase over 20 years rather than those of base case and sensitivity analysis scenarios.

Figure 7 depicts that using the analytical method for designing the cross-sectional area of the valve delays the water breakthrough time much more than other scenarios.

Cumulative water production using this analytical technique, at the end of the simulation period, was reduced by 90.7% compared to the worst scenario (the base case), and 56.5% in comparison with the GA's scenario.

As implied from Fig. 8, the injection flow rate in the highly permeable layer is well controlled by installing ICD with the cross-sectional area of the fluid flow obtained from the analytical technique. The injection rate to two layers (layers 8 and 9 of the field) was balanced by the proposed method which is quite comparable with the results obtained from GA, particularly in the second half of the reservoir's production life.

Based on the managerial approach of equalizing the velocity of the fluid in layers 8 and 9 of the field, breakthrough times for each layer in all 6 scenarios are plotted in Fig. 9. The time the water cut becomes greater than zero is the breakthrough time. As shown in Fig. 9, the breakthrough for the high-permeability layer (layer 9) occurs sooner for all scenarios, except in scenario 4 which is due to the extreme restriction of valve flow area (0.0001 ft²). For the high-permeability layer, breakthrough time increases from the base case scenario to scenarios 5 and 6, and then GA and analytical technique scenarios have higher amounts of water breakthrough time, respectively. For the low-permeability layer (layer 8), scenario 4 has the sooner water breakthrough time, and then the analytical technique and GA scenarios have higher breakthrough time values, respectively. After these three scenarios, there are scenarios 6, 5, and base case with higher breakthrough time values, respectively. It can be inferred that the three latter scenarios as well as scenario 4 are undesirable scenarios in which there is a considerable gap between the water breakthrough time of layers 8 and 9. On the other hand, in GA and analytical techniques, water breakthrough time values of layers 8 and 9 become closer together, which is advantageous for production and water handling.

As illustrated by black lines (solid and dotted-solid), the breakthrough time of the highly permeable layer is better delayed by using the analytical method in comparison with all other scenarios (except that of scenario 4 which is due to its extremely small valve size). Since the surface injection flow rate is constant, the injection rate in the low-permeability layer increases compared with the highly permeable layer (for equalizing velocities in two layers). As a result, the breakthrough time of the two layers becomes closer to each other (roughly synchronized), which is evident in the black curves of Fig. 9. Admittedly, the proposed method can effectively adjust the valve cross-sectional area so that water breakthrough time occurs simultaneously in different layers with different petrophysical characteristics. For cases other than analytical technique, breakthrough times for two layers are distinctly apart from each other, leading to early water production of the whole production system. In other words, although one layer contributes to water breakthrough later than the other one, the analytical technique

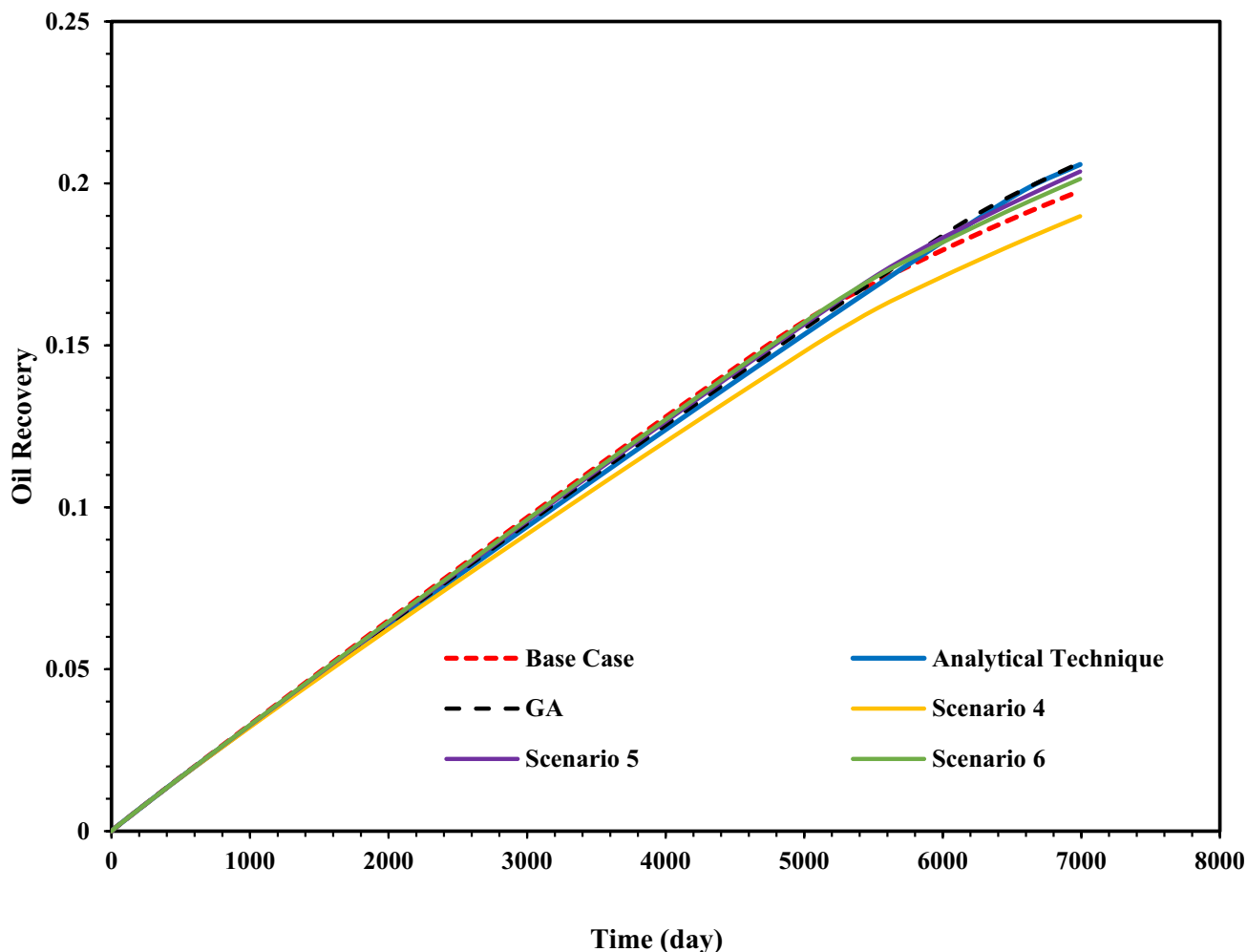


Fig. 6 Comparison of oil recovery in all scenarios

proves to be a more promising scenario for water production control (as confirmed in Fig. 7) owing to synchronizing the water breakthrough time of the high- and low-permeability layers. Early breakthrough of water even from one of the layers can put a stop to oil production from the other layer due to the emersion of a direct and conductive path for water from the injection well to the production one which mitigates the ability of the water to sweep oil from the less conductive layer. By delaying and synchronizing the breakthrough time of water of both layers, oil production would be higher, less water would be produced and the cost of water handling and separation would be reduced.

Figure 10 illustrates the NPV bar chart for all scenarios. To calculate NPV values, the oil price is considered as \$50 per barrel, injected water cost together with water handling expense are \$5 per barrel of oil produced, and the discount rate is 0.1. As demonstrated, GA shows the maximum NPV obtained for this study working based on its objective function which is NPV maximization. As a matter of fact,

although the proposed analytical method, by delaying the water breakthrough time, is of a significantly great amount of NPV (above \$274.8 million), that of the GA is marginally higher (less than \$276.6 million). The difference between the analytical and GA, NPVs seemingly is because the objective function of the latter is to optimize the NPV and that of the former is to delay water breakthrough time.

At last, all scenarios' results discussed above are collected in Table 4. In this table, oil recovery, cumulative water production, water breakthrough time, and NPV are shown for all scenarios of this study. All results were previously shown and discussed graphically, and this tabular form provides better insights for comparing each scenario's results. As shown, the most desirable value of each parameter is italicized. In the water breakthrough time column, results are classified for both the low-permeability layer (#8) and high-permeability layer (#9) together with the ratio of results for layer 8 to layer 9 (Table 5).

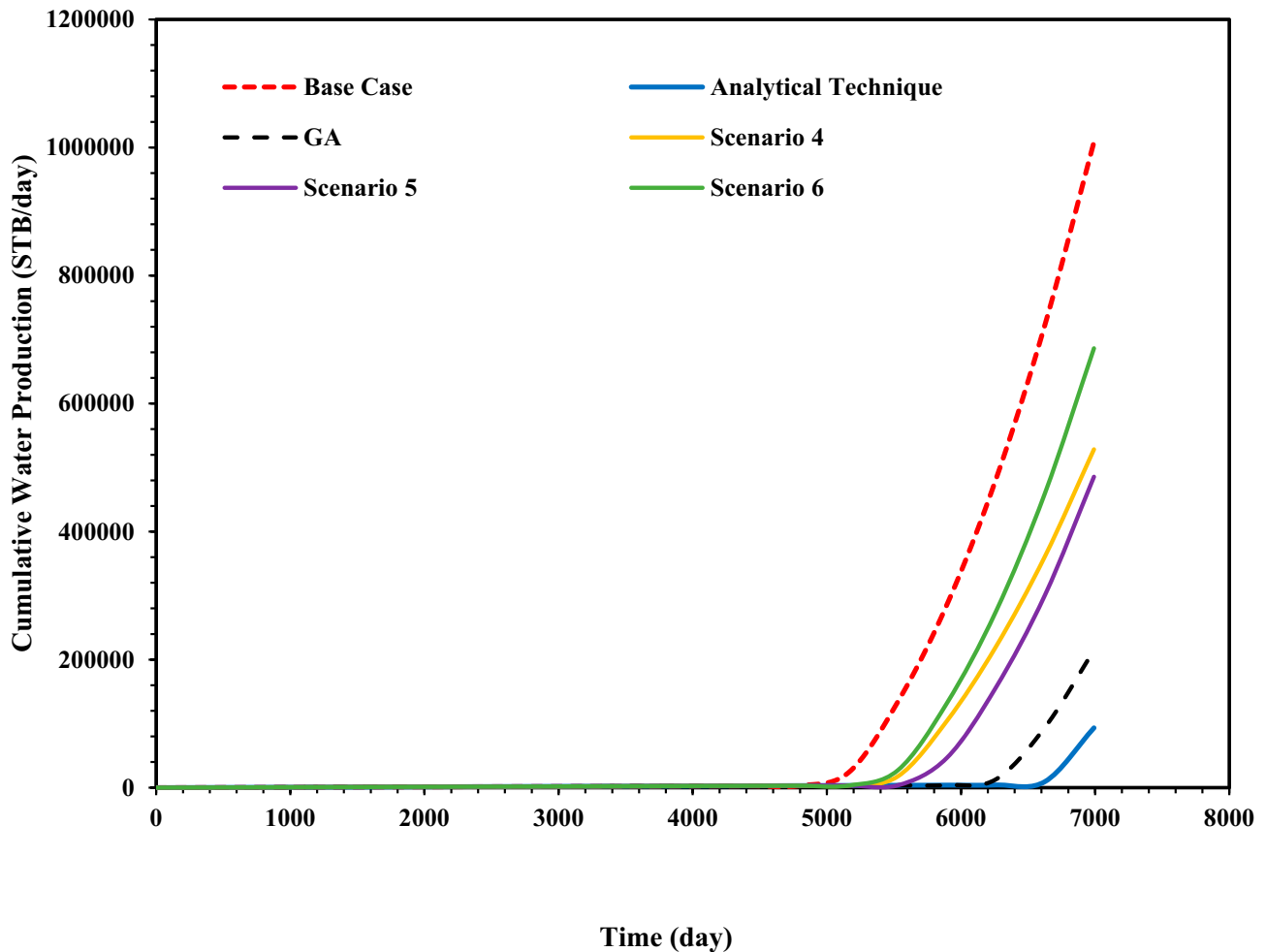


Fig. 7 Comparison of water breakthrough time in two scenarios

It is outlined that the genetic algorithm approach provides the most optimum results for the NPV and oil recovery, and the most desirable result for controlling water production and breakthrough time is for the analytical technique. GA and analytical method result in approximately 1.5% higher oil recovery compared with the worst-case scenario (#4). It is also evident that the analytical technique has been successful in synchronizing water breakthrough times in layers 8 and 9 with a near unity ratio of their water breakthrough time values (1.06). For the worst scenario (base case), the ratio of water breakthrough times in layers 8 and 9 is 1.76, which is not desirable for water production handling. As the analytical formulation of this study is not an optimization tool in nature and is a mathematical tool for fast ICD flow area determination, it can be inferred that this analytical technique outweighs all other scenarios. The reason is that it provides desirable results for water production control compared to all other scenarios as well as time-efficient, favorable results

for oil recovery and NPV comparable with those of the GA scenario.

Conclusions

A workflow was suggested based on reservoir simulation calculations which is coupled with a computational method of ICDs cross-sectional area quantification. An analytical formulation was presented in this study for ICD cross-sectional area determination. Based on this formulation, fluid movement in layers of a multi-layer reservoir with different properties was set to be balanced; accordingly, oil recovery increased, water breakthrough time was delayed, and cumulative water production was outstandingly reduced. Additionally, a genetic algorithm (GA) was utilized as an alternative approach, and a base case scenario (with no layer-scale inflow management of the valve) was employed alongside a sensitivity analysis regarding ICD's

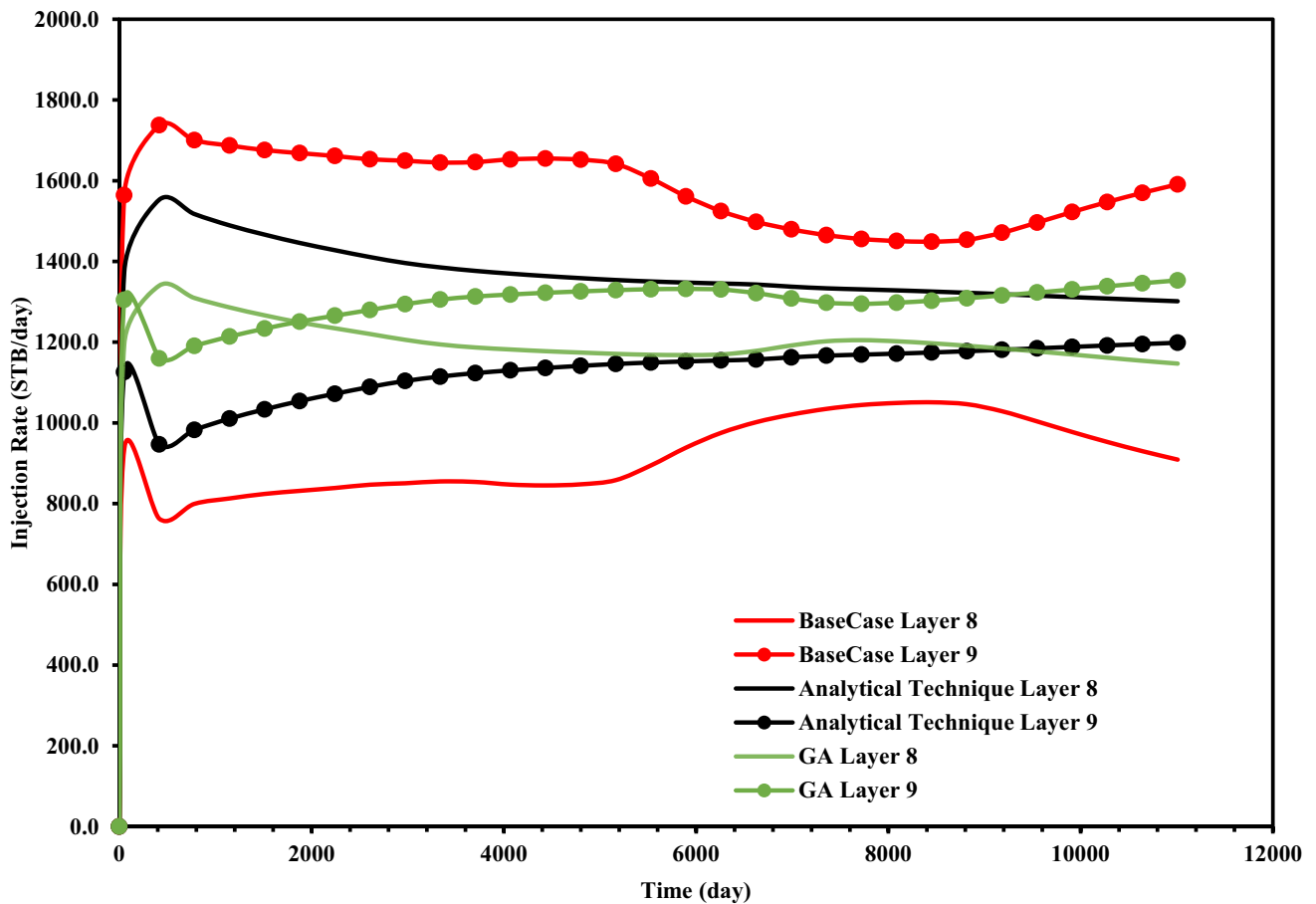


Fig. 8 Comparison of water injection rate in different layers in all scenarios

flow area for the sake of the analytical method and GA efficiency assessment in terms of oil production, water production, water injection rate, well water cut, and net present value (NPV). Accordingly, the most important conclusions drawn are as:

- Analytical technique determines ICD flow area with no reservoir simulation run and merely a closed-form formulation while other methods such as GA optimization and sensitivity analysis require iterative reservoir simulation runs.
- Analytical technique scenario provides desirable results with only one reservoir simulation run for obtaining field production and recovery results. In contrast, GA and sensitivity analysis scenarios obtain such results after multiple reservoir simulation runs for ICD flow area determination.
- The analytical method proposed outperforms the GA as it is less computationally demanding and provides better results for delaying water breakthrough time and lowering water production for the field data.
- The NPV calculated using the analytical technique and GA scenarios is greater than that of the base case scenario, which reveals the economic benefit of the analytical technique and GA methods to determine the cross-sectional area of the ICDs.

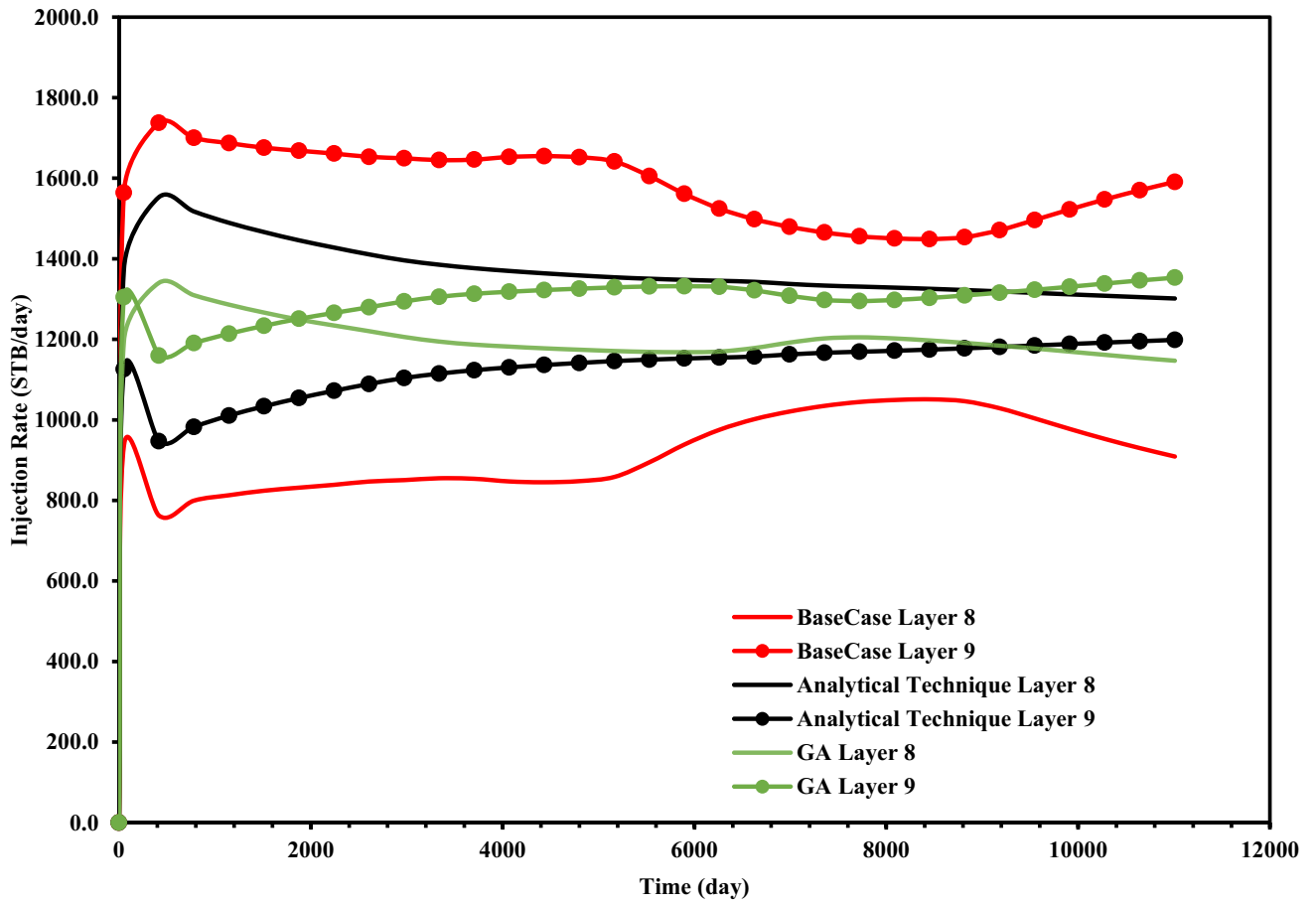


Fig. 9 Comparison of water breakthrough time of each layer in all scenarios

Fig. 10 NPV calculated for all the scenarios

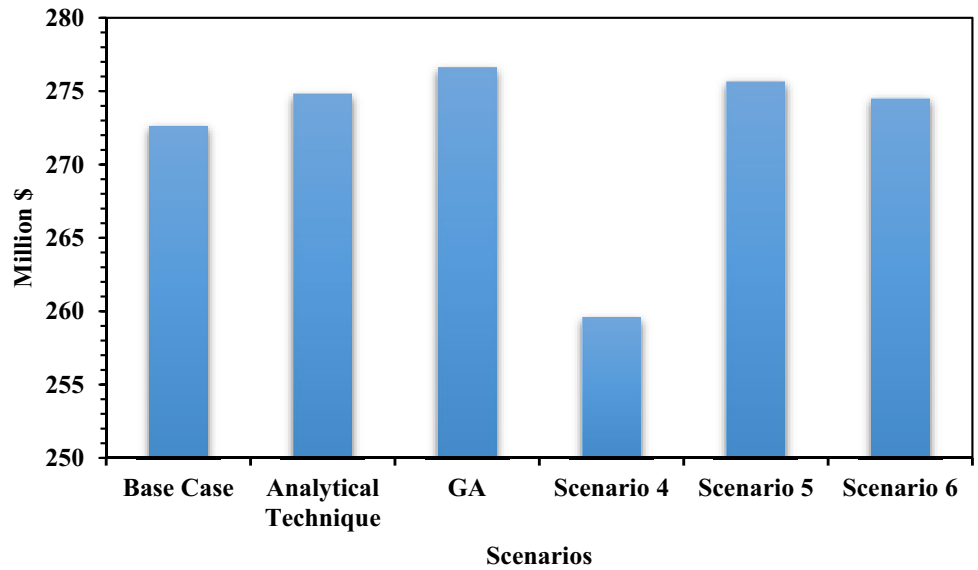


Table 4 Results for oil recovery, cumulative water production, water breakthrough time, and NPV of all scenarios

Scenario	Oil recovery (%)	Cumulative water production (STB)	Water breakthrough time (day)			NPV (million\$)
			Layer 8	Layer 9	Ratio	
Base case	19.77	1,008,390.8	8452	4799	1.76	272,605,949.7
Analytical technique	20.58	93,299.25	6626	6260	1.06	274,808,693.3
Genetic algorithm	20.64	214,497.28	6991	5895	1.19	276,595,420.6
Scenario 4	18.99	528,357.25	5165	9182	0.56	259,599,416.8
Scenario 5	20.37	485,536.31	7721	5165	1.49	275,641,734.5
Scenario 6	20.14	686,161.81	7356	5530	1.33	274,511,116

Table 5 General comparison of different cases results

Scenario	Computational efficiency	Data requirements	Performance
Base case	Single simulation run	Reservoir data	Poor NPV, Water production control and oil recovery
Analytical technique	Single simulation run	Reservoir data	Great NPV, Water production control and oil recovery
Genetic algorithm	Iterative simulation runs	Reservoir data	Great NPV and oil recovery but poor water production control
Scenario 4	Single simulation	Reservoir data	Poor NPV, Water production control, and oil recovery
Scenario 5	Single simulation	Reservoir data	Great NPV and oil recovery but poor water production control
Scenario 6	Single simulation	Reservoir data	Great NPV and oil recovery but poor water production control

Funding The authors declare that they have no relevant financial or non-financial interests to disclose.

Declarations

Conflict of interest The authors declare that they no conflict of interest.

Open Access This article is licensed under a Creative Commons Attribution 4.0 International License, which permits use, sharing, adaptation, distribution and reproduction in any medium or format, as long as you give appropriate credit to the original author(s) and the source, provide a link to the Creative Commons licence, and indicate if changes were made. The images or other third party material in this article are included in the article's Creative Commons licence, unless indicated otherwise in a credit line to the material. If material is not included in the article's Creative Commons licence and your intended use is not permitted by statutory regulation or exceeds the permitted use, you will need to obtain permission directly from the copyright holder. To view a copy of this licence, visit <http://creativecommons.org/licenses/by/4.0/>.

References

- Ahmed T (2018) Reservoir engineering handbook. Gulf Professional Publishing. <https://doi.org/10.1016/C2016-0-04718-6>
- Ahn S, Lee K, Choe J, Jeong D (2023) Numerical approach on production optimization of high water-cut well via advanced completion management using flow control valves. J Pet Explor Prod Technol 13(7):1611–1625. <https://doi.org/10.1007/s13202-023-01632-3>
- Al-Ghareeb ZM (2009) Monitoring and control of smart wells. Stanford University Stanford, California
- Alam MN, Das B, Pant V (2015) A comparative study of metaheuristic optimization approaches for directional overcurrent relays coordination. Electric Power Syst Res 128:39–52. <https://doi.org/10.1016/j.epsr.2015.06.018>
- Aljbran M, Horne R (2020) Prediction of multilateral inflow control valve flow performance using machine learning. SPE Prod Oper 35(03):691–702. <https://doi.org/10.2118/196003-PA>
- Asadollahi M (2012) Waterflooding optimization for improved reservoir management. Norwegian University of Science Technology
- Behrouz T, Rasaei MR, Masoudi R (2016) A novel integrated approach to oil production optimization and limiting the water cut using intelligent well concept: using case studies. Iran J Oil Gas Sci Technol 5(1):27–41. <https://doi.org/10.22050/ijogst.2016.13827>
- Brouwer DR, Jansen JD, van der Starre S, van Kruijsdijk CPJW, Berentsen CWJ (2001) Recovery increase through water flooding with smart well technology. In: SPE-68979-MS. SPE European formation damage conference. <https://doi.org/10.2118/68979-MS>
- Chen B, Reynolds AC (2017) Optimal control of ICV's and well operating conditions for the water-alternating-gas injection process. J Pet Sci Eng 149:623–640. <https://doi.org/10.1016/j.petrol.2016.11.004>
- Chu H, Zhang J, Zhang L, Ma T, Gao Y, Lee WJ (2023) A new semi-analytical flow model for multi-branch well testing in natural gas hydrates. Adv Geo-Energy Res 7(3):176–188. <https://doi.org/10.46690/ager.2023.03.04>
- Cullick AS, Sukkestad T (2010). Smart operations with intelligent well systems. In: SPE-126246-MS. SPE intelligent energy conference and exhibition. <https://doi.org/10.2118/126246-MS>
- Dan XU, Ruilin HU, Wei GAO, Jiaguo XIA (2015) Effects of laminated structure on hydraulic fracture propagation in shale. Pet Explor Dev 42(4):573–579. [https://doi.org/10.1016/S1876-3804\(15\)30052-5](https://doi.org/10.1016/S1876-3804(15)30052-5)
- Dejam M, Hassanzadeh H (2022) Dispersion tensor in stratified porous media. Phys Rev E 105(6):65115. <https://doi.org/10.1103/PhysRevE.105.065115>
- Dutt A, Mandal A (2012) Modified analytical model for prediction of steam flood performance. J Pet Explor Prod Technol 2(3):117–123. <https://doi.org/10.1007/s13202-012-0027-9>

- Ebadi F, Davies DR (2006) Should proactive or reactive control be chosen for intelligent well management?. In: SPE-99929-MS. Intelligent energy conference and exhibition. <https://doi.org/10.2118/99929-MS>
- Ebadi F, Davies DR, Reynolds MA, Corbett PWM (2005) Screening of reservoir types for optimisation of intelligent well design, SPE-94053-MS. In: SPE Europec/EAGE Annual Conference
- Eltaher E, Muradov K, Davies D, Grassick P (2019) Autonomous flow control device modelling and completion optimisation. *J Pet Sci Eng* 177:995–1009. <https://doi.org/10.1016/j.petrol.2018.07.042>
- Gao CH, Rajeswaran RT, Nakagawa EY (2007) A literature review on smart well technology, SPE-106011-MS. Production and operations symposium. <https://doi.org/10.2118/106011-MS>
- Hassanabadi M, Motahhari SM, Nadri Pari M (2012) Optimization of ICDs' port sizes in smart wells using particle swarm optimization (PSO) algorithm through neural network modeling. *J Chem Pet Eng* 46(2):97–109. <https://doi.org/10.22059/jchpe.2012.2388>
- Huang G, Ma H, Hu X, Cai J, Li J, Luo H, Pan H (2019) A coupled model of two-phase fluid flow and heat transfer to transient temperature distribution and seepage characteristics for water-flooding production well with multiple pay zones. In: *Energies*, vol 12, issue 10. <https://doi.org/10.3390/en12101854>
- Kalam S, Yousuf U, Abu-Khamsin SA, Waheed UB, Khan RA (2022) An ANN model to predict oil recovery from a 5-spot waterflood of a heterogeneous reservoir. *J Pet Sci Eng* 210:110012. <https://doi.org/10.1016/j.petrol.2021.110012>
- Karkevandi-Talkhooncheh A, Hajirezaie S, Hemmati-Sarapardeh A, Husein MM, Karan K, Sharifi M (2017) Application of adaptive neuro fuzzy interface system optimized with evolutionary algorithms for modeling CO₂-crude oil minimum miscibility pressure. *Fuel* 205:34–45. <https://doi.org/10.1016/j.fuel.2017.05.026>
- Lee B, Faizal SA, Galimzyanov A (2017) An innovative ICD design workflow to balance flux equalization and well productivity in horizontal wells, SPE-183957-MS. In: SPE middle east oil & gas show and conference. <https://doi.org/10.2118/183957-MS>
- Li L, Huang B, Tan Y, Deng X, Li Y, Zheng H (2017) Geometric heterogeneity of continental shale in the Yanchang Formation, Southern Ordos Basin. *Sci Rep*. <https://doi.org/10.1038/s41598-017-05144-z>
- Li Z, Fernandes P, Zhu D (2011) Understanding the roles of inflow-control devices in optimizing horizontal-well performance. *SPE Drill Complet* 26(03):376–385. <https://doi.org/10.2118/124677-PA>
- Meshioye O, Mackay E, Ekeoma E, Chukuwezi M (2010) Optimization of waterflooding using smart well technology, SPE-136996-MS. In: Nigeria annual international conference and exhibition. <https://doi.org/10.2118/136996-MS>
- Meum P, Tøndel P, Godhavn J-M, Aamo OM (2008) Optimization of smart well production through nonlinear model predictive control, SPE-112100-MS. In: Intelligent energy conference and exhibition. <https://doi.org/10.2118/112100-MS>
- Mohammadi Behboud M, Ramezanzadeh A, Tokhmechi B, Mehrad M, Davoodi S (2023) Estimation of geomechanical rock characteristics from specific energy data using combination of wavelet transform with ANFIS-PSO algorithm. *J Pet Explor Prod Technol* 13(8):1715–1740. <https://doi.org/10.1007/s13202-023-01644-z>
- Mohammadpourmarzbali S, Rafiei Y, Fahimpour J (2019) Improved waterflood performance by employing permanent down-dole control devices: Iran case study. In: Youth technical sessions proceedings, 1st ed., pp 333–339. CRC Press
- Moradi A, Moldestad BME (2020) Near-well simulation of oil production from a horizontal well with ICD and AICD completions in the Johan Sverdrup field using OLGA/ROCX. In: Proceedings of The 61st SIMS Conference on Simulation and Modelling SIMS 2020, September 22–24, Virtual Conference, Finland, 249–256. <https://doi.org/10.3384/ecp20176249>
- Mostakhdeminhosseini F, Rezvani H, Rafiei Y (2020) A novel analytical technique for ICD design in a waterflood project: iran case study. In: EAGE 2020 annual conference & exhibition online, 2020, pp 1–5. <https://doi.org/10.3997/2214-4609.202010973>
- Perkins TK (1993) Critical and subcritical flow of multiphase mixtures through chokes. *SPE Drill Complet* 8(04):271–276. <https://doi.org/10.2118/20633-PA>
- Prakasa B, Muradov K, Davies D (2019) Principles of rapid design of an inflow control device completion in homogeneous and heterogeneous reservoirs using type curves. *J Pet Sci Eng* 176:862–879. <https://doi.org/10.1016/j.petrol.2019.01.104>
- Rafiei Y (2014) Improved oil production and waterflood performance by water allocation management. Heriot-Watt University
- Rahimbakhsh A, Rafiei Y (2018) Investigating the effect of employing inflow control devices on the injection well on the SAGD process efficiency using an integrated production modeling. SPE-190407-MS. In: SPE EOR conference at oil and gas West Asia. <https://doi.org/10.2118/190407-MS>
- Rezvani H, Rafiei Y (2023) A novel analytical technique for determining inflow control devices flow area in CO₂-EOR and CCUS projects. *J Pet Explor Prod Technol* 13(9):1951–1962. <https://doi.org/10.1007/s13202-023-01654-x>
- Sabet N, Irani M, Hassanzadeh H (2022) Inflow control devices placement: a computational fluid dynamics approach. *SPE J* 27(03):1562–1576. <https://doi.org/10.2118/209211-PA>
- Schlumberger (2010) ECLIPSE reference manual. Schlumberger
- Taghavinejad A, Brown C, Ostadhassan M, Liu B, Hadavimoghaddam F, Sharifi M (2022) A real-world impact of offset frac-hits by rate transient analysis in the Bakken and Three Forks, North Dakota, USA. *J Petrol Sci Eng* 208:109710. <https://doi.org/10.1016/J.PETROL.2021.109710>
- Ugwu AA, Moldestad BME (2018) The application of inflow control device for an improved oil recovery using ECLIPSE. In: Proceedings of The 9th EUROSIM congress on modelling and simulation, EUROSIM 2016, The 57th SIMS Conference on Simulation and Modelling SIMS 2016, 142, pp 694–699. <https://doi.org/10.3384/ecp17142694>
- Wang J, Liu H, Liu Y, Jiao Y, Wu J, Kang A (2016) Mechanism and sensitivity analysis of an inflow control devices (ICDs) for reducing water production in heterogeneous oil reservoir with bottom water. *J Pet Sci Eng* 146:971–982. <https://doi.org/10.1016/j.petrol.2016.08.007>
- Wang L, Zhou H, Wang J, Yu R, Cai J (2021) Semi-analytical model for pumping tests in discretely fractured aquifers. *J Hydrol* 593:125737. <https://doi.org/10.1016/j.jhydrol.2020.125737>
- Xiaorong L, Likuan Z, Yuhong L, Caizhi H, Hui S, Binfeng C (2016) Structural heterogeneity of reservoirs and its implication on hydrocarbon accumulation in deep zones. *China Pet Explor* 21(1):1–10
- Zhang N, Li H, Liu Y, Shan J, Tan Y, Li Y (2019) A new autonomous inflow control device designed for a loose sand oil reservoir with bottom water. *J Pet Sci Eng* 178:344–355. <https://doi.org/10.1016/j.petrol.2019.03.034>
- Zhang R, Zhang Z, Li Z, Jia Z, Yang B, Zhang J, Zhang C, Zhang G, Yu S (2021) A multi-objective optimization method of inflow control device configuration. *J Pet Sci Eng* 205:108855. <https://doi.org/10.1016/j.petrol.2021.108855>

Publisher's Note Springer Nature remains neutral with regard to jurisdictional claims in published maps and institutional affiliations.